CATHENA MODEL OF THE END SHIELD COOLING SYSTEM FOR POINT LEPREAU GENERATING STATION

F. Caracas[*], M. Maltchevski[*], V. Lau[*], L. Sun[**]
[*]Atomic Energy of Canada, Limited, Sheridan Science and Technology Park, Mississauga, Ontario, L5K 1B2
[**]NB Power, Point Lepreau Generating Station, P.O. Box 600, Lepreau, New Brunswick, E5J 2S6

Abstract:
Failures in the shield cooling system (i.e. loss of circulation, loss of heat sink and loss of end shield inventory) cause the metal components in the end shield assembly to heat up. These components, particularly the inner and outer tubesheets, heat up at different rates. Thermal loading of the tubesheets in this manner causes them to deform and possibly lead to distortion of the calandria assembly and exert extra load on the fuel channels. This in turn may jeopardize the integrity of the fuel channels and/or operation of the shutdown systems.

This paper discusses the CATHENA thermalhydraulic model of the end shield cooling system used in Point Lepreau. The thermalhydraulic response of the system following different Point Lepreau Generating Station transients and the predicted system temperature are also presented.

The thermalhydraulic response of the system following shield cooling system failures and the temperature profile of the inner and outer calandria tubesheets can be obtained using this model. Such tubesheet differential temperatures are normally used as input to assess the integrity of the calandria assembly following postulated end shield cooling system failures.

Acknowledgements
The authors of this paper would like to thank Bruce Hanna of Atomic Energy of Canada Limited for his valuable comments in preparing the model for end shield cooling system.

1. INTRODUCTION

The end shield cooling system removes heat, which accumulates in the calandria vault, and end shields due to nuclear heating from the reactor core and heat transfer from the fuel channels, heat transport system feeders, and moderator. The other main function of this system is to maintain the calandria vault and end shields full of water to provide biological shielding against radiation during normal operation and shutdown conditions. Failures in the end shield cooling system (i.e. loss of circulation, loss of heat sink and loss of end shield inventory) cause the metal components in the end shield assembly to heat up. These components, particularly the inner and outer tubesheets, heat up at different rates. Thermal loading of the tubesheets in this manner causes them to deform and possibly lead to distortion of the calandria assembly and exert extra load on the fuel channels. This in turn may jeopardize the integrity of the fuel channels and/or operation of the shutdown systems.

In order to predict the differential temperature between the calandria (inner) and fuelling machine (outer) tubesheets a thermal and a hydraulic model of the shield cooling system was developed. The CATHENA model developed for the end shield cooling system takes into account the heat load to the system and the system hydraulics. A description of the model and major assumptions is presented in the following sections.

A number of simulations were performed to test the model robustness and adequacy to model the end shield cooling system. The design system parameters such as pressures, temperatures and flows were reproduced based on a steady state simulation.

The comparison with **P**oint **L**epreau **G**enerating **S**tation (PLGS) plant measured data following a power run-down and run-up transients is presented.

A parameter sensitivity study was also performed to assess the effect of using different values for heat transfer coefficient and hydraulic diameter in the end shield region on the predictions of the maximum differential temperature between the inner and outer calandria tubesheets. The results of the parameter sensitivity study are also presented.

2. MODEL DESCRIPTION AND ASSUMPTIONS

The end shield cooling system model was developed to analyse postulated end shield cooling system failures. The objective of such analysis is to predict the differential temperature between the inner and outer tubesheets in order to determine if the potential exists for differential tubesheet deformation. Excessive deformation could damage fuel channels and/or shutoff rod assemblies.

The end shield cooling system model was developed such to provide a conservative estimate of temperature differences between the two tubesheets. This is achieved by the combination of assuming high heat load to the end shield and a low moderator temperature. Furthermore, the model assumes that the maximum heat is generated in the inner tubesheets and no heat is generated in the outer tubesheets. This set of assumptions takes into account the operating conditions prior and after the reactor trip.

The hydraulic model was developed to provide the hydraulic information in different locations of the circuit, which is used by the thermal model to predict the metal temperatures in axial and radial directions along the end shield structures (i.e., inner/outer tubesheet, steel balls and lattice tubes).

The end shield cooling system noncondensable gases are modelled as saturated steam, and applying the numeric option to disable condensation. The tee junctions in the circuit piping are modelled as CATHENA volume components.

The thermal model was developed to predict the wall metal temperature based on the heat transfer coefficient between the fluid and metal structures (i.e., inner/outer tubesheet, steel balls and lattice tubes). The heat transfer correlations are determined based on average fluid velocity.

The CATHENA **GEN**eralized **H**eat **T**ransfer **P**ackage (GENHTP) was used to model the heat transfer in the end shield tubesheets, carbon steel balls and lattice tubes with the internal heat sources where applicable. The heat sources model the direct neutronic and gamma heating of the specific metal structure as the reactor operates at full power.

2.1 CATHENA Hydraulic Model

The schematic diagram of the end shield cooling system is presented in Figure 1 and includes the major components of the system:

- A 100% operating pump (PUMP1). The shield cooling system has two 100% pumps but only one is running during normal operation and the other one is on standby,
- Two 50% capacity heat exchangers for heat removal (HX1 and HX2),
- The two end shields X and Y (ENDSHX and ENDSHY),
- The calandria vault including the cover gas space above (CVAULT),
- The two delay tanks (TK1 and TK2),
- The head tank (TK3),
- The purification circuit including the ion exchanger
- Air piping and rupture discs (two 6-inch and one 24-inch rupture discs, RD-1, 2 and RD-3 respectively),

The end shield rings are not modelled separately. They serve to keep the concrete temperature of the calandria vault structure within the design limits. The flow through the end shield rings does not contribute directly to the cooling inside the end shield

structure. As a result, it does not have influence on the stress of the end shield tubesheets. The coolant flow going through the rings is added to the calandria vault inlet flow.
The detailed piping geometry was input from the available Point Lepreau isometric "as-built" drawings. The minor losses and friction factors were determined from Reference [1]. The end shield cooling system hydraulic model was fine tuned to achieve the design flow distribution under normal operation by varying the area of restriction orifices located at different points of the hydraulic circuit, similar to the process performed during commissioning. The CATHENA model represents the restriction orifices as valves.

Pumps
Only one 100% capacity pump was modelled (identified as PUMP1 in the model). No pump switchover was modelled during transient simulation because the analysis scenario of the loss of flow end shield cooling system (ESCS) failure does not include the restart of the stand-by pump. As a result, the stand-by pump is not represented in the CATHENA model.

Heat Exchangers
The model represents each heat exchanger separately. The inlet and outlet piping as well as heat exchanger tubes are modelled as CATHENA pipe components. The end shield cooling system 50% capacity heat exchangers HX1 and HX2 are modelled as simple heat input boundary conditions.

End Shields X and Y
The end shields X and Y are modelled separately. The connecting pipes are modelled according to the "as-built" isometric drawings to accurately represent the differences in the circuit geometry between the two end shields. The end shield X and Y inlet piping is represented by pipe components ENDSHXEN and ENDSHYEN respectively. The end shield themselves are modelled by pipe components ENDSHX and ENDSHY. The hydraulic resistance of the end shield carbon balls is calculated as the resistance of a packed bed assuming the design 60/40-volume ratio of steel balls to surrounding water. The ENDSHX and ENDSHY pipe components are represented with 22 nodes, one per each row of fuel channels, to provide a detailed pressure drop calculation. The end shield X and Y outlet piping is modelled as pipe components ENDSHXEX and ENDSHYEX respectively.

Calandria Vault (Shield Tank)
The calandria vault is modelled as a tank component with the variable cross section area to account for the vertical geometry changes. The heat added to the vault water from the calandria shell and the neutron and gamma radiation is modelled using a tank heater. The nitrogen supply system is modelled via a boundary condition N2SUPP. The connecting valve opens once the cover gas pressure falls below the low cover gas pressure setpoint and closes once the pressure reaches the high cover gas pressure alarm setpoint. The valve area is adjusted to limit the maximum N_2 flow to 20 L/sec. The nitrogen supply system model can be disabled, if needed. There is also a new 24-inch rupture disc

connected to the calandria vault (RD-3). The rupture disc RD-3 is connected to a boundary condition reservoir component RDATM.

Delay Tanks TK-1 and TK-2

The delay tanks are identical. They are modelled as 4 pipe components connected in series. TK1-1 and TK2-1 represent the tank inlets. The annular space is modelled as TK1-2 and TK2-2 and the inner downcomer pipes are modelled as TK1-3 and TK2-3 with the corresponding cross section areas and hydraulic diameters. The outlet parts of the tanks are represented as TK1-4 and TK2-4 respectively.

Ion Exchanger Circuit

The ion exchanger circuit is represented by the following pipe components: 3W20, IX and 3W19. The restriction orifice RO-9 is modelled as a valve. The valve open fraction is adjusted to achieve the design flow through the ion exchanger circuit.

Air Piping And Rupture Discs

The air and water pipes connected to the existing rupture discs RD-1 and RD-2 are modelled in great detail. These are usually small diameter pipes ranging from 3/4 to 6 inch. They are represented as pipe components. The rupture discs open once the differential pressure exceeds 69 kPa(g). The discharge is directed to a boundary condition reservoir component RBATM. The rupture discs are modelled as valves.

Break Lines

Four different break circuits are modelled. These elements do not exist in the real plant. They are modelled to simulate the following accident sequences:

- 12W7-BR1, 12W7-BR2 connected to the boundary condition reservoir component DBLBRK. This circuit models a double-ended guillotine break of the largest end shield cooling system 12-inch pipe. This break location leads to a simultaneous total inventory loss from the both end shields. The check valves V-29 and V-36 are assumed stuck open. At time zero, valve V-12W7BR is closed and valves V-12W7B1 and V-12W7B2 are open.
- 10W13BR1, 10W13BR2 are connected to the boundary condition reservoir component SGLBRKX. This break location allows modelling a single or double-ended break of the end shield X inlet header.
- 10W7BR1, 10W7BR2 are connected to the boundary condition reservoir component SGLBRKY. This break location allows modelling a single or double-ended break of the end shield Y inlet header.
- HX1BRK, HX2BRK are connected to the boundary condition reservoir component HXBRK. This break location allows modelling of a single HX pipe break in either heat exchanger or both.

End Shield Cross-Section Area and Hydraulic Diameter

The end shield cross-section area varies greatly in the vertical direction reaching a maximum at the middle plane. The end shield is modelled as a CATHENA pipe component to account for the flow resistance associated with the internal components. The pipe component does not allow for the cross-section area variation with height.

Hence, a representative flow area and hydraulic diameter have been selected. In order to calculate the average representative flow area and hydraulic diameter, the following methodology was used. For each channel row a number of parameters were determined (details in Figure 2):

- Number of lattice tubes in a row $N_{row\ LT}$, -
- Length L of the channel row, m
- Total cross-section flow area is calculated as: $A_{tot} = L \cdot L_{TS}$, m^2, where L_{TS} is the distance between the tubesheets, m
- Cross-section area taken by the lattice tubes: $A_{LT} = d_{out} \cdot L_{TS} \cdot N_{row\ LT}$, m^2, where d_{out} is the outer diameter of the lattice tubes, m
  $N_{row\ LT}$ is the number of lattice tubes in a row, -
- Cross-section area available for the coolant flow: $A_{free} = A_{tot} - A_{LT}$, m^2
- Actual flow area was determined assuming 60% is occupied by the shielding balls: $A_{actual} = 0.4 \times A_{free}$, m^2
- Wetted perimeter: P_{wet}, m
- Hydraulic diameter: $D_{hyd} = 4 \cdot A_{actual} / P_{wet}$, m

After averaging the values for the flow area and the hydraulic diameter over each row, the values for a representative row are obtained. The flow area and the hydraulic diameter of the end shield component are set to the values for a representative row. In addition, the fluid volume in the end shield was preserved using the design metal to water ratio of 60/40 that corresponds to the ratio between the carbon steel balls and the end shield liquid.

Minor Losses Coefficient in the Shielding Balls Region

The end shield inner volume is filled with carbon steel shielding balls. The flow through this area is considered as a flow in a packed bed. To obtain the pressure drop through a packed bed, the following relation is used, References [2], [3]:

$$\Delta P = f_p \frac{L}{D_p} \rho V_s^2 \frac{1-\varepsilon}{\varepsilon^3} \qquad (1)$$

Where:

f_p – friction factor, -
L – height of the packed bed, m
D_p – steel ball diameter, m
ρ – fluid density, kg/m^3
V_s – superficial velocity, m/sec
ε – liquid fraction in the packed bed ($\varepsilon = 0.4$), -

To calculate the value of f_p, it is necessary to determine the Reynolds number. The relation for Re_p, Reference [3], can be written as follows:

$$\mathrm{Re}_p = \frac{\rho D_p V_s}{(1-\varepsilon)\mu} \qquad (2)$$

Where:

μ – dynamic viscosity of liquid, Pa · sec

For $Re_p > 1000$ (fully turbulent flow), the Burke-Plummer equation can be used with $f_p = 1.75$ (Reference [3]). Substituting $f_p = 1.75$ into equation (1) and comparing it with the

Darcy formula for the pressure drop calculation (3), one arrives at the following relation for K (4):

$$\Delta P = f_p \frac{L}{D_p} \frac{\rho V_s^2}{2} \qquad \text{(Darcy formula)} \tag{3}$$

$$K = 3.5 \frac{1-\varepsilon}{\varepsilon^3} \tag{4}$$

Hence, K = 3.5 (1 – 0.4) / 0.4^3 = 32.8125.

2.2 CATHENA Thermal Model

The end shields are cylindrical vessels bounded at the ends by the inner and outer tubesheets. Each end shield is filled with coolant (demineralised water) and carbon steel shielding balls. Lattice tubes penetrate each end shield and span the distance between the inner and outer tubesheets. Coolant enters each end shield at the bottom and exits from the top.

Nuclear heating of the shielding balls, lattice tubes, and tubesheets is not uniform across the face of the end shields. Heat is transferred to the end shield coolant from the PHT fuel channels (via the lattice tubes) and heat from nuclear radiation generated in carbon steel balls/water regions, thermal shields and structures outside end shields or transferred to calandria shell and inner tubesheets. The temperature of the PHT coolant is not uniform along the channels. The temperature of the moderator is not uniform across the face of the inner tubesheets.

Complex heat generation and heat transfer mechanisms occur within the end shields. In the current model, the detailed local hydraulic behaviour cannot be simulated since CATHENA can only model 1-D fluid flow. The impact of using the average velocity provided by a 1-D fluid flow instead of a multidimensional fluid flow is not significant, since the model is intended to predict the average volumetric metal temperatures in the end shield inner and outer tubesheets over the transients that last tens of minutes and even hours. The spatial variations of the temperatures in fluid and solid components within the end shield space are not very large and do not greatly affect the overall metal stresses, which are the function of average volumetric metal temperatures.

Several assumptions are made with respect to the heat generation and heat transfer between the various end shield metal components in order to obtain conservative metal temperature transients while modeling with reasonable accuracy the system response and event timing.

The end shield thermal model assumptions are discussed below:

A. Four heat transfer models have been used to model the heat transfer to end shield fluid from different components of the end shield system. The heat transfer models take advantage of the calandria assembly symmetry.
   - A model representing the heat transfer between the shielding balls and the end shield water.
   - A model representing the heat transfer between the PHT coolant, lattice tubes and the end shield water.
   - A model representing the heat transfer between the inner calandria tubesheets and the end shield coolant.

- A model representing the heat transfer between the outer calandria tubesheets and the end shield coolant.

B. No heat transfer by conduction is modeled between the different heat transfer models (e.g., no heat transfer between the lattice tubes and tubesheets). This assumption will maximize the heat load to the end shield water. The heat transfer by conduction between the different heat transfer models is not significant for the end shield tubesheets temperature distribution.

C. The axial heat conduction along the length of the heat transfer models is neglected. This approach will maximize the temperature gradients in the heat transfer models. The axial heat conduction along the length of the heat transfer models has little impact on end shield tubesheets temperature distribution because the heat models are represented by multiple nodes transferring the heat to the end shield water by forced convection.

Radiation heat transfer between heat transfer models was not modeled, as it is insignificant at low temperature.

Heat Transfer Coefficient Correlations

The default set of CATHENA heat transfer correlations was used for all GENHTP models except for the lattice tube and shielding ball regions. No condensation on the heat transfer surfaces was modelled.

For the lattice tube and shielding ball regions, the Zukauskas (cross-flow) liquid convective heat transfer correlation was selected since the flow in the end shield region is over the shielding balls and across the lattice tubes. There are 22 rows of lattice tubes in the end shields. The correlation was developed for forced convection heat transfer flow across tube bundles of at least 10 rows deep, Reference [4]. The correlation is verified for a variety of in-line and staggered tube bundle configurations for Re numbers ranging from 10^3 to 10^6 and system pressures ranging from 660 Pa(a) to 22 MPa(a), which envelopes the end shield cooling system conditions.

Carbon Steel Shielding Balls Model

WENDSHX1 and WENDSHY1 are the carbon steel shielding balls GENHTP models for the end shields X and Y respectively. Adiabatic boundary conditions are used on the inner surface of the shielding balls. The outside surface of the shielding balls is facing the end shield water. The total mass, volume and heat transfer area of the shielding balls are conserved. The built-in CATHENA material properties for carbon steel are used. The internal heat source due to the neutron and gamma radiation is modelled in the shielding balls (Reference [5]).

Lattice Tubes and Fuel Channels Model

WENDSHX2 and WENDSHY2 are the lattice tubes and fuel channels GENHTP models for the end shields X and Y respectively. The lattice tubes are located horizontally inside the end shields with the end shield coolant flow going across them in the vertical direction, Figure 2. The fuel channels are inside the lattice tubes. The total mass, volume and heat transfer area of the lattice tubes are conserved. The built-in CATHENA material properties for stainless steel are used. The boundary conditions on the inside of the fuel channels are modelled as a function of the primary heat transport (PHT) coolant temperature and heat transfer coefficient. The gap conductivity between the fuel channels and the lattice tubes is adjusted to transfer the designed amount of heat from the PHT coolant to the end shield water (Reference [5]). The outside surface of the lattice tubes is facing the end shield water. No internal heat source due to the neutron and gamma radiation is modelled in the lattice tubes.

Inner Tubesheet Model

WENDSHX3 and WENDSHY3 are the inner tubesheets GENHTP models for the end shields X and Y respectively. The total mass, volume and heat transfer area of the inner tubesheet are conserved. The built-in CATHENA material properties for stainless steel are used. The boundary conditions on the inside of the inner tubesheet are modelled as a function of the moderator temperature and heat transfer coefficient, which is adjusted to transfer the design amount of heat to the end shield water and to the moderator (Reference [5]). The internal heat source due to the neutron and gamma radiation is modelled in the inner tubesheet (Reference [5]). The outside surface of the inner tubesheet is facing the end shield water.

Outer Tubesheet Model

WENDSHX4 and WENDSHY4 are the outer tubesheets GENHTP models for the end shields X and Y respectively. The total mass, volume and heat transfer area of the outer tubesheet are conserved. The built-in CATHENA material properties for stainless steel are used. The boundary conditions on the outside of the outer tubesheet are modelled as a function of the feeder cabinet air temperature and heat transfer coefficient, which is adjusted to obtain the design average temperature in the outer tubesheet metal. No internal heat source due to the neutron and gamma radiation is modelled in the outer tubesheet (Reference [5]). The inside surface of the outer tubesheet is facing the end shield water.

3. COMPARISON TO PLANT DATA

Point Lepreau Generating Station provided some plant data to compare the end shield model predictions with the measured plant parameters. The speed of these plant transients, in the order of tens of minutes or even hours, is similar to the progression of scenarios for which the current model is built to analyse.

3.1 Verification Against PLGS Power Run-down Transient

Introduction
As part of the end shield model verification exercise, PLGS provided the measurements for the plant power run-down transient that took place on April 6, 2007, from 21:00:00 to 23:00:00. The data was provided using an Excel file and included the following information:

- Relative reactor power,
- End shield inlet temperature (63411-TT15, AI 730), ºC,
- End shield X outlet temperature (63411-TT07, AI 2740), ºC,
- End shield Y outlet temperature (63411-TT08, AI 2741), ºC,
- Calandria vault outlet temperature (63411-TT09, AI 2742), ºC,
- Calandria vault cover gas pressure (63411-PT19, AI 2743), kPa(g),
- Calandria vault water level (63411-LT21, AI 2744), mm.

Description of the Transient
The reactor power was kept constant at about 91.05% FP for the first hour of operation from 09:00:00 PM to 10:00:00 PM (3600 sec), Figure 3. The power was reduced in a series of steps to about 77% FP at 10:04:48 PM (3888 sec). Then at approx. 10:17:42 PM (4662 sec) the reactor was shutdown and remained at the decay power level until the end of the transient at 11:00:00 PM (7200 sec).

Discussion of Results
Overall, the CATHENA model predictions agree well with the measured parameters. The CATHENA model did not simulate the calandria vault inlet temperature controller. The heat removal in the heat exchangers was modelled as a simple constant boundary condition. The end shield heat load in the model assumed no PHT temperature reduction due to the reactor trip. The PHT heat load contribution through the fuel channels remained constant, even though the reactor power decreased to the decay heat levels. The steady state end shield inlet and outlet coolant temperature were slightly higher than the measured values, Figure 4 and Figure 5. The predicted end shield inlet coolant temperature decreased faster than the measured one, Figure 4, following the reactor trip due to the discussed above simplified heat removal boundary condition in the heat exchangers. The end shield outlet coolant temperature was in a fairly good agreement with the measured values, Figure 5.

Summary
The CATHENA model predicted the power run-down transient recorded at the PLGS on April 6, 2007 with a reasonable degree of accuracy. The margin of deviation between the calculated and measured parameters was small. The model did not simulate any PHT

cooldown following the reactor trip, though the provided measurement data suggested that the PHT temperature started to decrease shortly after the reactor shutdown. The end shield inlet and outlet coolant temperatures were in a good agreement with the plant data and consistent with the higher simulated heat load in the model and a simplified constant heat removal boundary condition in the heat exchangers.

3.2 Verification Against PLGS Power Run-up Transient

Introduction
PLGS provided the measurements for a plant power run-up transient that took place on May 3, 2007, from 01:00:00 to 08:00:00. Some of the data provided in the Excel file format included:

- Relative reactor power,
- End shield inlet temperature (63411-TT15, AI 730), ºC,
- End shield X outlet temperature (63411-TT07, AI 2740), ºC,
- End shield Y outlet temperature (63411-TT08, AI 2741), ºC,
- Calandria vault outlet temperature (63411-TT09, AI 2742), ºC,
- Calandria vault cover gas pressure (63411-PT19, AI 2743), kPa(g),
- Calandria vault water level (63411-LT21, AI 2744), mm.

Description of the Transient
The reactor power was kept constant at about 51.03% FP for the first 46 minutes 42 seconds of operation from 01:00:00 AM to 01:46:42 AM (2802 sec), Figure 6. The power then was increased to about 67% FP at 01:52:24 AM (3144 sec). It stayed at this level for about 26 minutes until 02:18:06 AM (4686 sec). Then the power was reduced again to approx. 51% FP level at 02:23:42 AM (5022 sec). The reactor operated at this level for about 2 hours 47 minutes until 05:10:54 AM (15054 sec). Finally, in a series of steps, the power was increased to approx. 82% FP at 05:43:36 AM (17016 sec) where it was kept constant until the end of the transient.

Discussion of Results
Overall, the CATHENA model predictions agree well with the measured parameters. The steady state end shields inlet and outlet coolant temperatures were approx. one degree higher than the measured values, Figure 7 and Figure 8. The predicted values were in a fairly good agreement with the measurements, following the recorded trends closely.

Summary
The CATHENA model predicted the power run-up transient recorded at the PLGS on May 3, 2007 with a reasonable degree of accuracy. The margin of deviation between the calculated and measured parameters was small. The end shield inlet and outlet coolant temperatures were in a good agreement with the plant data and consistent with the higher simulated heat load in the model. Overall, the model captured the temperature and level trends recorded in the power run up transient correctly.

4. END SHIELD MODEL PARAMETER SENSITIVITY STUDY

In addition to comparison of the model predictions with the plant transients and design parameters, a sensitivity study was conducted to determine the model sensitivity to the different values for hydraulic diameter in the end shield and for the **h**eat **t**ransfer **c**oefficient (HTC). A comparison between the HTC predicted by the end shield cooling system CATHENA model and the HTC under free convection conditions has also been performed.

4.1 Description of Methodology

The variation of the CATHENA predicted HTC for the lattice tubes and shielding balls was achieved through setting the multiplier "CORRECTION FACTOR" to an appropriate value. The base case had the "CORRECTION FACTOR" of 1.0, i.e., no correction to the predicted HTC value. The hydraulic diameter was varied in the input file for the ENDSHX and ENDSHY components.

A selected set of transients was run first with the base input file (the original hydraulic diameter, HTC Correction Factor = 1.0) and then with the following parameter variations:

- HTC Correction Factor for the Lattice Tube and Shielding Ball GENHTP Models was set to 1.50 (50% increase over the value calculated by CATHENA). The end shield hydraulic diameter was not changed from the original value.
- HTC Correction Factor for the Lattice Tube and Shielding Ball GENHTP Models was set to 0.50 (50% decrease over the value calculated by CATHENA). The end shield hydraulic diameter was not changed from the original value.
- The end shield hydraulic diameter was increased by 50% from the original value. HTC Correction Factor for the Lattice Tube and Shielding Ball GENHTP Models was not changed (1.0).
- The end shield hydraulic diameter was decreased by 50% from the original value. HTC Correction Factor for the Lattice Tube and Shielding Ball GENHTP Models was not changed (1.0).
- The end shield hydraulic diameter was decreased tenfold (-1000%) from the original value. This made the end shield hydraulic diameter closer to the diameter of a shielding ball. HTC Correction Factor for the Lattice Tube and Shielding Ball GENHTP Models was increased tenfold (+1000%).

4.2 Discussion of Results

The results of the performed analyses demonstrated that the maximum temperature differential (ΔT_{max}) between the end shield inner and outer tubesheets was largely insensitive to the ±50% or even +1000% variation in the HTC and ±50% variation in the hydraulic diameter. The maximum variation of ΔT_{max} versus the base case (the original hydraulic diameter, HTC Correction Factor = 1.0) ranged from –3.71ºC to +2.96ºC.

A comparison between the HTC predicted by the end shield cooling CATHENA model and the HTC under free convection conditions shows that the HTC calculated by CATHENA is conservative.

5. CONCLUSION

This paper has documented the CATHENA thermalhydraulic model of the Point Lepreau end shield cooling system.

The comparison between PLGS plant measured data following a power run-down and run-up transients and model simulation results shows that the model predicts the thermalhydraulic parameters with reasonable degree of accuracy.

The parameter sensitivity study results clearly demonstrate that the maximum predicted temperature differential between the tubesheets is largely insensitive to ±50% or even much larger variation in the heat transfer coefficient and ±50% variation in the hydraulic diameter. A comparison between the HTC predicted by the end shield cooling CATHENA model and the HTC under free convection conditions shows that the HTC calculated by CATHENA is conservative.

The thermalhydraulic response and the average volumetric metal temperature profile of the inner and outer calandria tubesheets of the end shield cooling system following postulated failures can be obtained using this model. The tubesheet differential temperatures can be used as input to assess the integrity of the calandria assembly following postulated end shield cooling system failures.

To complement the verification work performed using Point Lepreau plant transient data, future model development and validation work is planned using the moderator and end shield system heat transfer experiments performed at AECL.

6. REFERENCES

[1] Flow of Fluids through Valves, Fittings, and Pipe. Metric Edition - SI Units, Technical Paper No. 410M, CRANE Co., 1986

[2] Perry, R. H. and Green, D., Perry's Chemical Engineers' Handbook, 6th. Ed., McGraw-Hill, New York, 1986

[3] W.E. McCabe, J.C. Smith, and P. Harriott "Unit Operations of Chemical Engineering", McGraw-Hill, New York, 2001

[4] A. Zukauskas, "Heat transfer from tubes in cross-flow", Advances in Heat Transfer Vol.8, pp. 93-160, 1972

[5] K. Aydogdu, "Moderator-System And Shield-Cooling System Heat Loads After Reactor Shutdown For CANDU 6 Reactors", 25th Annual Conference of the Canadian Nuclear Society, Toronto, Ontario, Canada, June 6-9, 2004.

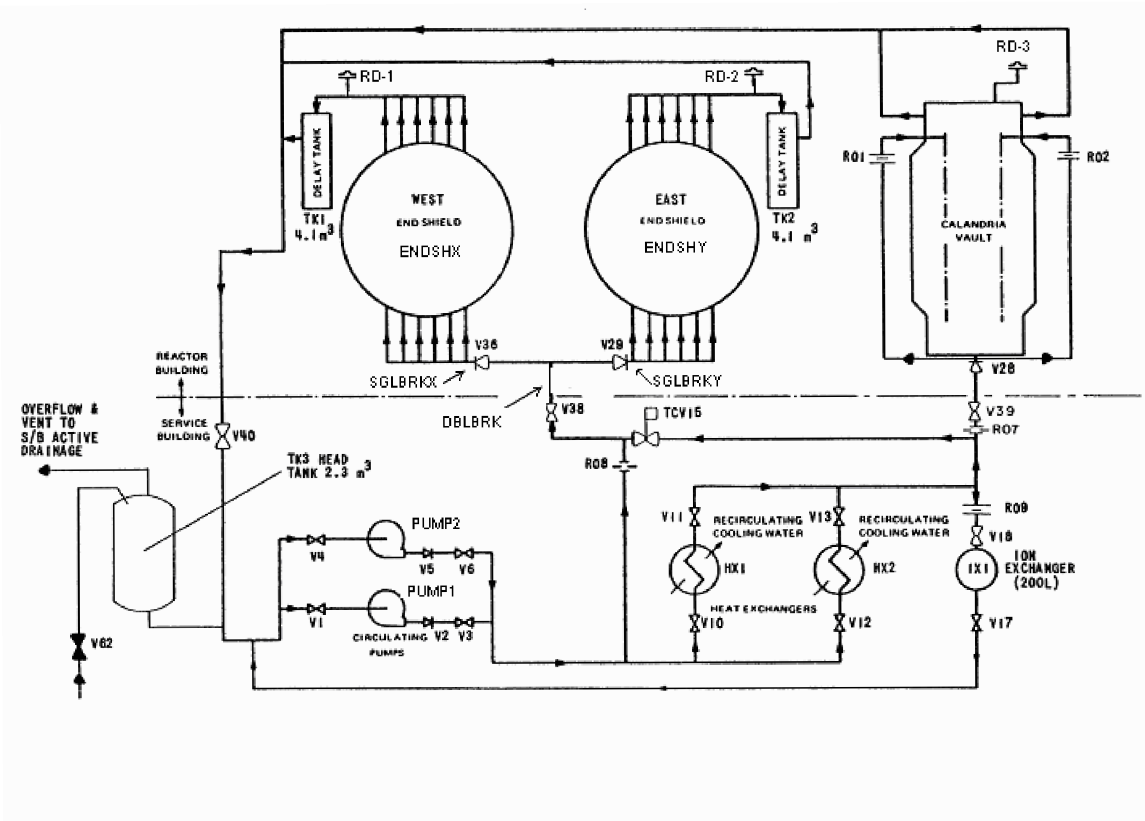

Figure 1 End Shield Cooling System Schematic Diagram

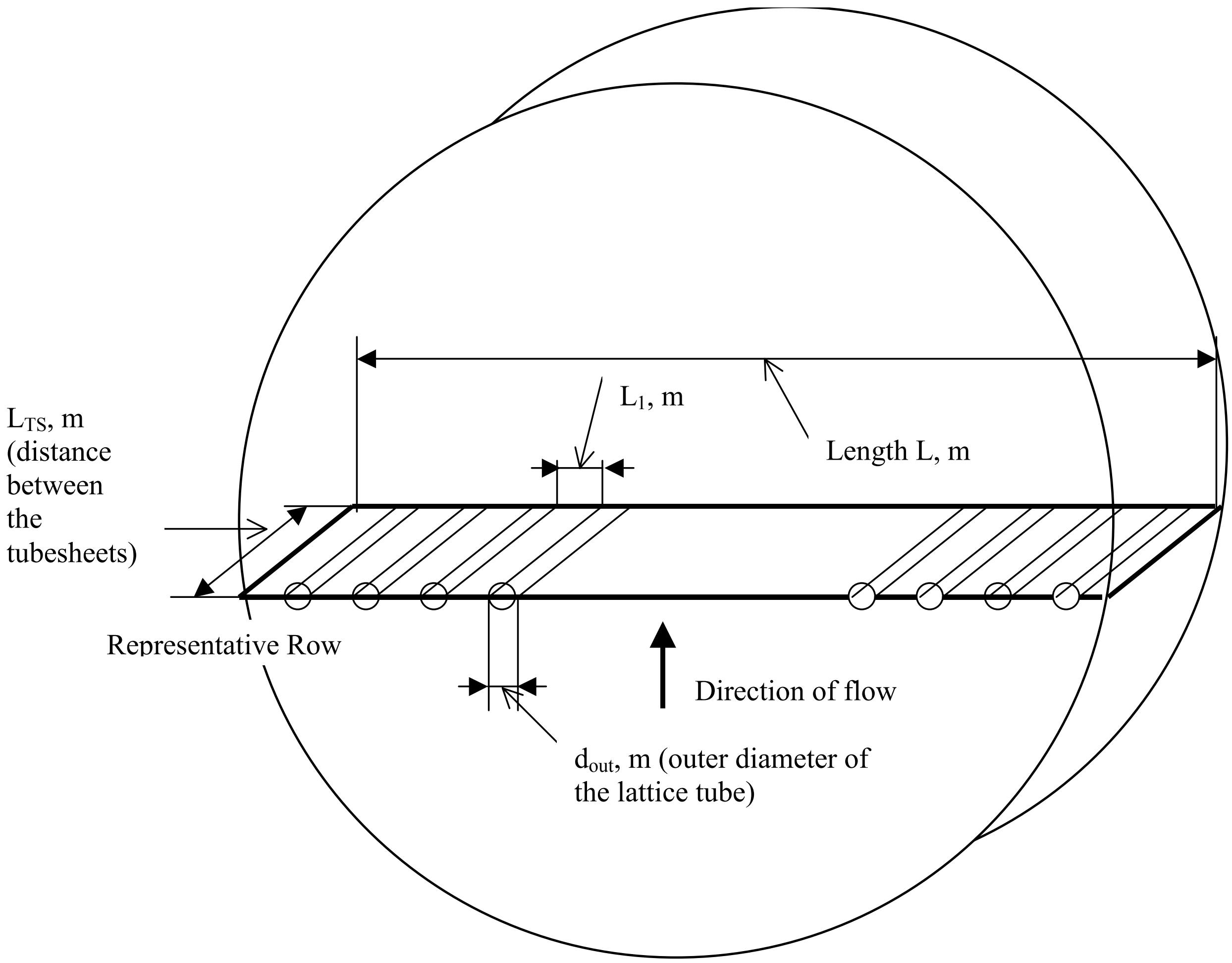

Figure 2 The End Shield Region Wetted Perimeter and Hydraulic Diameter

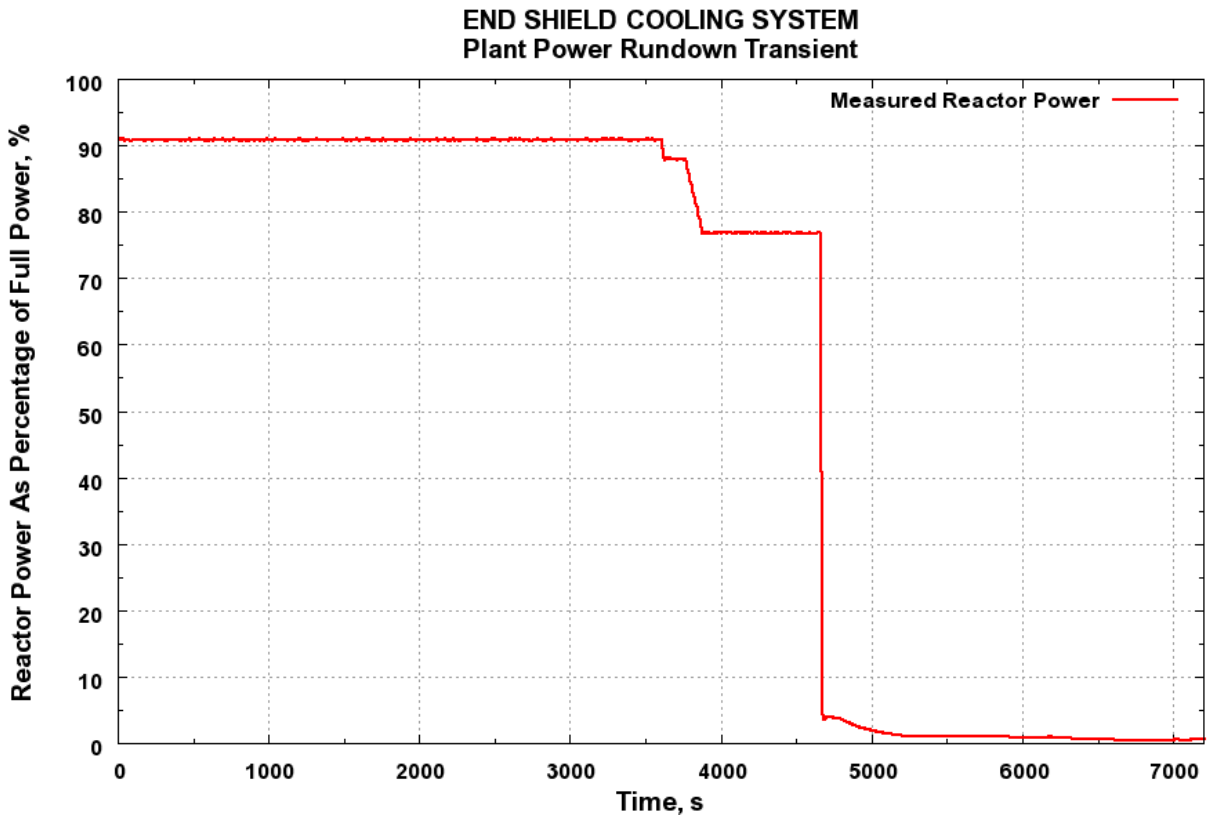

Figure 3 Measured Reactor Power (Power Run-down)

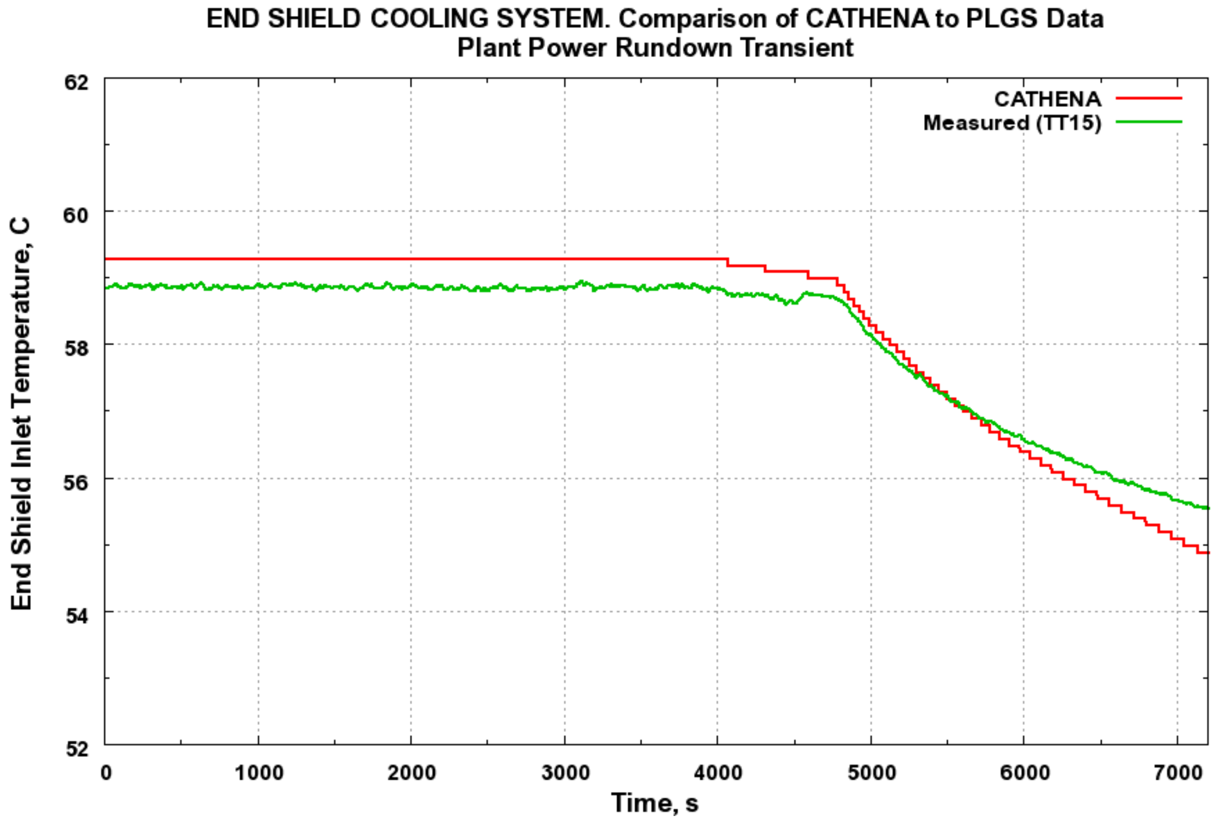

Figure 4 End Shield X and Y Inlet Coolant Temperatures (Power Run-down)

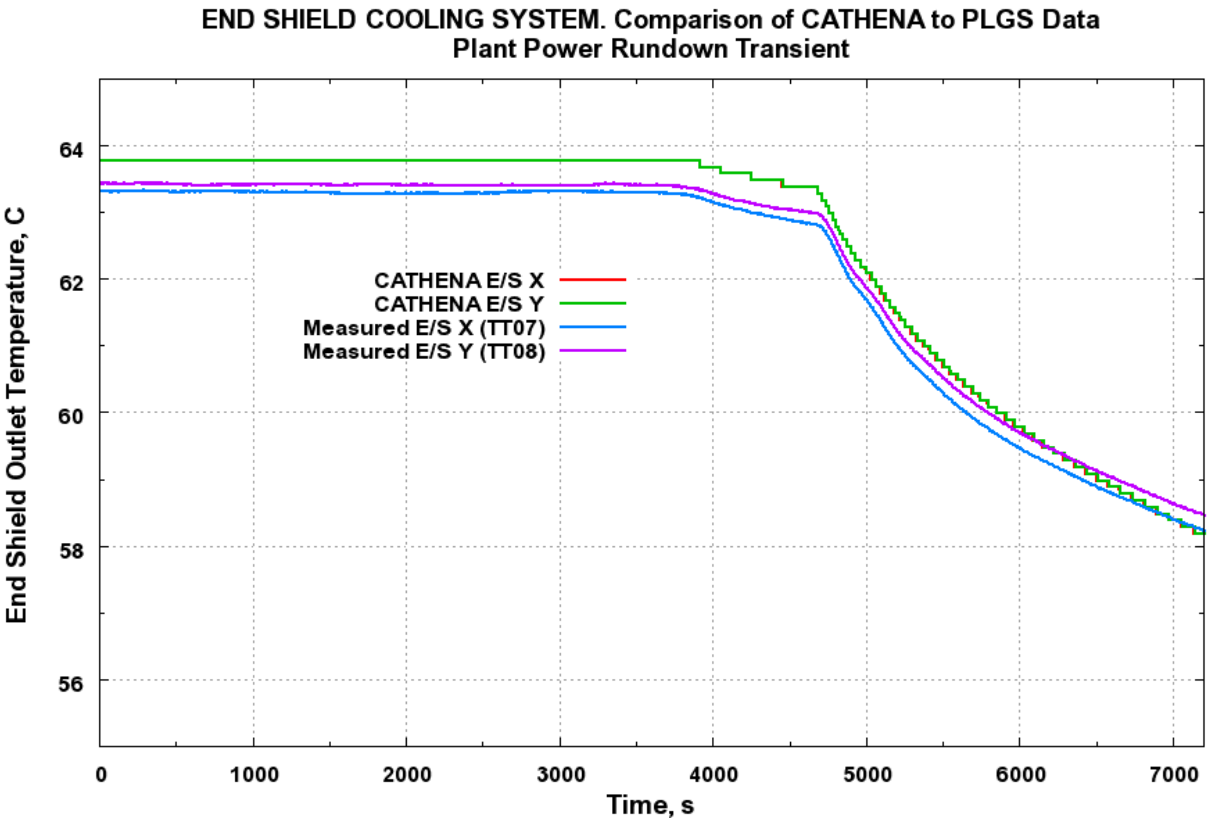

Figure 5 End Shield X and Y Outlet Coolant Temperatures (Power Run-down)

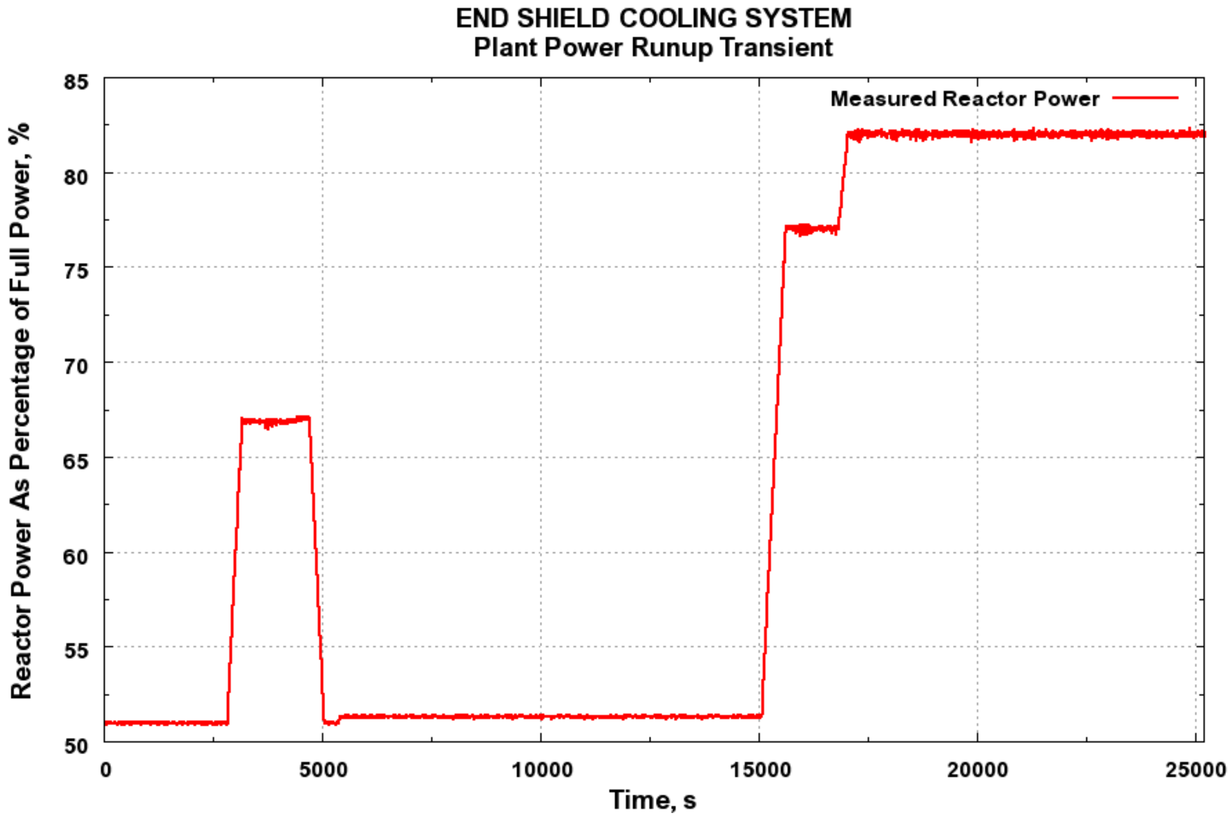

Figure 6 Measured Reactor Power (Power Run-up)

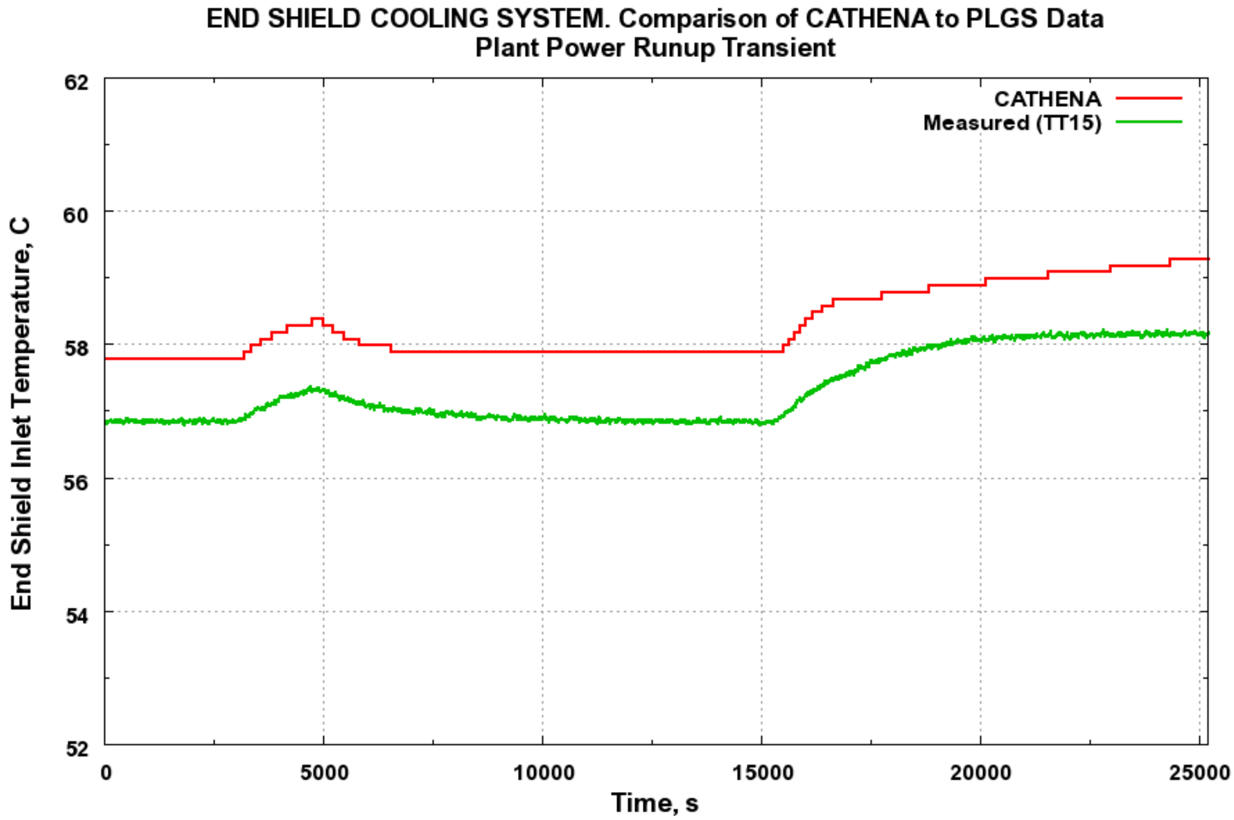

Figure 7 End Shield X and Y Inlet Coolant Temperatures (Power Run-up)

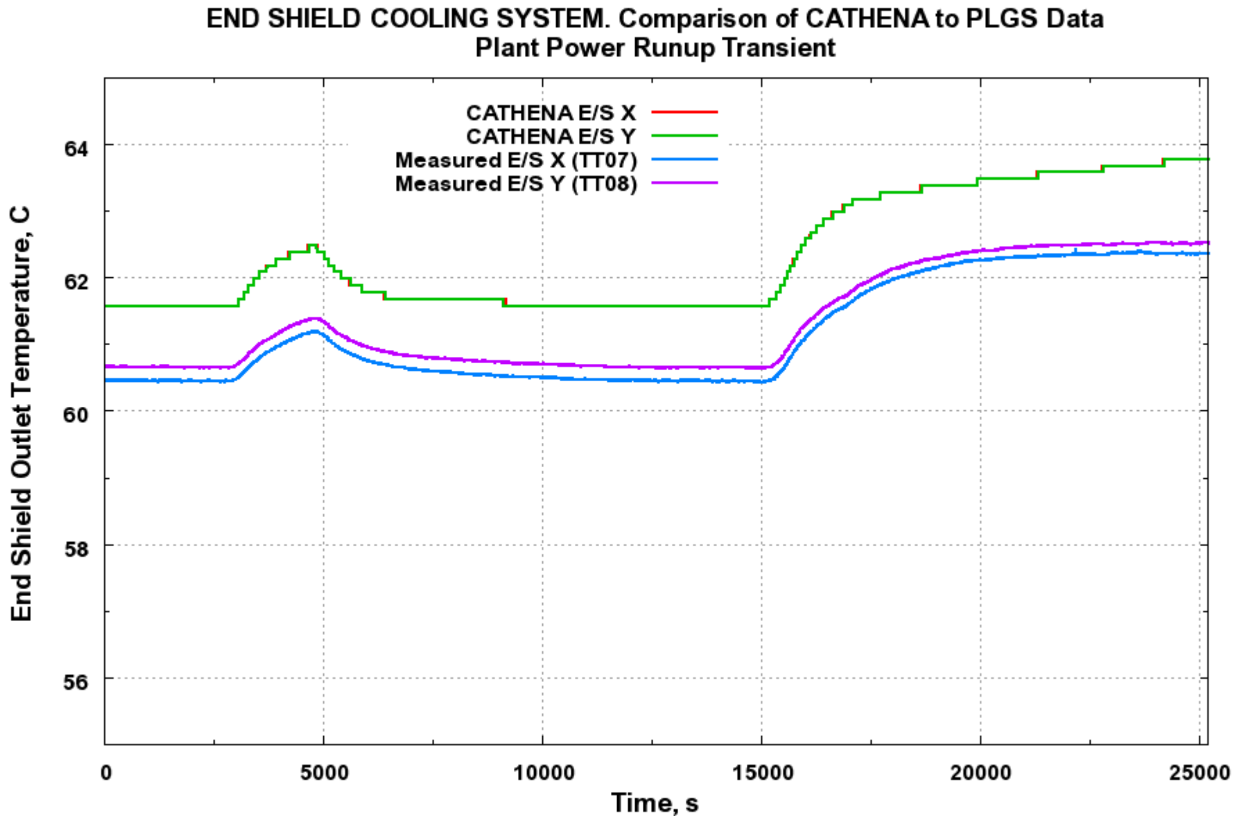

Figure 8 End Shield X and Y Outlet Coolant Temperature (Power Run-up)